

# Reentrant superfluidity and pair density wave in single-component dipolar Fermi gases

Yanming Che, Jibiao Wang, and Qijin Chen\*

Zhejiang Institute of Modern Physics and Department of Physics, Zhejiang University, Hangzhou, Zhejiang 310027, China  
and Synergetic Innovation Center of Quantum Information and Quantum Physics, Hefei, Anhui 230026, China

(Received 21 December 2015; revised manuscript received 23 May 2016; published 10 June 2016)

We study the superfluidity of single-component dipolar Fermi gases in three dimensions using a pairing fluctuation theory, within the context of BCS-BEC crossover. The transition temperature  $T_c$  for the dominant  $p_z$  wave superfluidity exhibits a remarkable reentrant behavior as a function of the pairing strength induced by the dipole-dipole interaction (DDI), which leads to an anisotropic pair dispersion. The anisotropy and the long-range nature of the DDI cause  $T_c$  to vanish for a narrow range of intermediate interaction strengths, where a pair density wave emerges as the ground state. The superfluid density and thermodynamics below  $T_c$ , along with the density profiles in a harmonic trap, are investigated as well. Implications for experiments are discussed.

DOI: [10.1103/PhysRevA.93.063611](https://doi.org/10.1103/PhysRevA.93.063611)

## I. INTRODUCTION

The recent experimental realization of quantum degenerate Fermi gases of magnetic atoms [1–3] and the rapid progress toward creating degenerate polar molecules [4–6] have opened a new frontier for exploring novel phases of quantum gases, where dipole-dipole interaction (DDI) plays a central role. A lot of attention has been paid to unconventional  $p$ -wave superfluids [7–11] in three dimensions (3D) and topological superfluids [12] in two dimensions (2D). The latter has been associated with Majorana fermions and can be used for topological quantum computation [13]. Such exotic superfluid phases emerge from the long-range DDI with a strong anisotropy, which differs from the widely studied contact potential in dilute atomic gases. Moreover, the relative DDI strength can be tuned by changing the fermion number density  $n$  (or Fermi wave vector  $k_F$ ) and, in the case of polar molecules [14], by varying an external electric field strength.

Of particular interest is the intermediate pairing strength regime, where complex physics beyond the weak-coupling BCS theory arises and the superfluid transition temperature  $T_c$  is relatively high, making it more practical to access the superfluid phase experimentally. For a contact potential, the entire BCS–Bose-Einstein condensation (BEC) crossover from weak- to strong-coupling regimes has been studied intensively in two-component Fermi gases of  $^6\text{Li}$  or  $^{40}\text{K}$ . In contrast, such a crossover in dipolar Fermi gases, where richer physics may arise, is yet to be explored. Existing theoretical studies in this aspect mostly focus on the ground state, based on mean-field treatments [7,8,15,16], which are inadequate in addressing moderate and strong-coupling regimes at finite temperature.

In this paper, we address the superfluidity and pairing phenomena of *single-component* dipolar Fermi gases in 3D, with an emphasis on the finite temperature and interaction effects. Built on previous work [17,18] that has been applied successfully to address various BCS-BEC crossover phenomena in two-component Fermi gases with a contact interaction [18,19], here we construct a similar pairing fluctuation theory for the superfluidity of fully polarized *one-component* dipolar

fermions (in the  $\hat{z}$  direction), in which thermally excited pairs naturally give rise to a pseudogap in the fermion excitation spectrum. We find that (i) the DDI leads dominantly to a  $p_z$ -wave superfluid, and the superfluid  $T_c$  curve exhibits a reentrant behavior as a function of the DDI strength; in the intermediate regime of the BCS-BEC crossover,  $T_c$  vanishes and the ground state becomes a pair density wave (PDW), similar to the PDW state studied in underdoped high- $T_c$  superconductors [20,21]. (ii) In the fermionic regime, the temperature dependence of superfluid density and low  $T$  thermodynamic quantities exhibit power laws, as expected but in stark contrast to the contact interaction case [22]. (iii) Within a local density approximation (LDA), the density profile in an isotropic harmonic trap exhibits a similar qualitative behavior to its  $s$ -wave counterpart, despite the different pairing symmetry and the anisotropic pair mass.

The emergence of the PDW state originates from the long-range nature of the DDI, which essentially put the system in the high density regime. The  $p_z$ -wave symmetry leads further to a nonlocal effect [23] and hence a diverging coherence length in the nodal  $xy$  plane, *which makes it difficult for the pairs to move in the  $\hat{z}$  direction, without heavily colliding with each other*. At certain intermediate pairing strengths, the interaction energy between pairs may dominate the kinetic energy, in favor of forming a Wigner-like crystal in the  $\hat{z}$  direction. This PDW state may exhibit behaviors of a Bose metal [24,25], with a Bose “surface” for pair excitations at a finite pair momentum  $q_z$  (with  $q_x = q_y = 0$ ). The two dimensionality of the pair dispersion in the remaining  $xy$  plane destroys possible long-range superfluid order, leading to a metallic ground state with a density wave of Cooper pairs in the  $\hat{z}$  direction.

## II. THEORETICAL FORMALISM

We consider an ultracold gas of one-component dipolar fermions of mass  $m$  in unit volume, with dipole moment  $\mathbf{d} = d\hat{z}$ , fully polarized in the  $\hat{z}$  direction. We follow the pairing fluctuation theory as described in Ref. [17], with fermion energy  $\xi_{\mathbf{k}} = \mathbf{k}^2/(2m) - \mu$  measured with respect to the chemical potential  $\mu$  (we take  $\hbar = k_B = 1$ , as usual). We shall write the pairing interaction  $V_{\mathbf{k},\mathbf{k}'}$  into an effective separable form [26], i.e.,  $V_{\mathbf{k},\mathbf{k}'} = g\varphi_{\mathbf{k}}\varphi_{\mathbf{k}'}^*$ , where  $g$  is the pairing

\*Corresponding author: qchen@zju.edu.cn

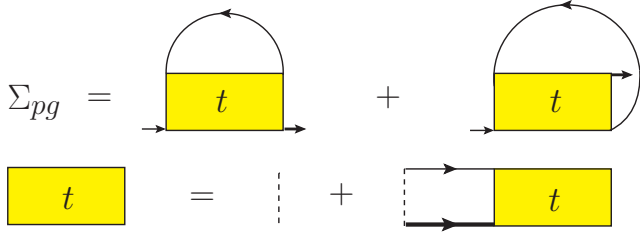


FIG. 1. Feynman diagrams for the pairing fluctuation self-energy  $\Sigma_{pg}$  and  $T$  matrix  $t$ . The thin solid, thick solid, and dashed lines represent the bare propagator  $G_0$ , dressed propagator  $G$ , and DDI, respectively.

strength, and  $\varphi_{\mathbf{k}}$  is the symmetry factor with an odd parity and will be determined by the DDI.

Following previous work [17,27,28], the fermion self-energy comes from particle-particle scattering, which leads to both an order parameter (below  $T_c$ ) and a pseudogap. Noncondensed pairs are treated on an equal footing with single particle propagators. In contrast to the  $s$ -wave singlet pairing case [17], an extra exchange diagram has now been retained in the self-energy, as shown in Fig. 1. Besides the pairing symmetry, this exchange diagram is a major difference between singlet and triplet pairing. Therefore, we obtain the fermion self-energy from noncondensed pairs

$$\begin{aligned}\Sigma_{pg}(K) &= \Sigma_{pg}^{\text{direct}}(K) + \Sigma_{pg}^{\text{exchange}}(K) \\ &= \sum_{Q \neq 0} t(Q) G_0(Q-K) \varphi_{\mathbf{k}-\mathbf{q}/2} \varphi_{\mathbf{k}-\mathbf{q}/2}^* \\ &\quad - \sum_{Q \neq 0} t(Q) G_0(Q-K) \varphi_{\mathbf{k}-\mathbf{q}/2} \varphi_{3\mathbf{q}/2-\mathbf{k}}^*,\end{aligned}\quad (1)$$

where  $t(Q) = 1/[g^{-1} + \chi(Q)]$ , with  $\chi(Q) = \sum_K G(K) G_0(Q-K) |\varphi_{\mathbf{k}-\mathbf{q}/2}|^2$ , and  $G_0$  ( $G$ ) the bare (full) fermion Green's function. Below  $T_c$ , the condensate self-energy is

$$\Sigma_{sc}(K) = -\Delta_{sc}^2 G_0(-K) |\varphi_{\mathbf{k}}|^2, \quad (2)$$

as in BCS theory, with the superfluid order parameter  $\Delta_{sc}$ . As in Ref. [17], we use a four-vector notation,  $K \equiv (i\omega_n, \mathbf{k})$ ,  $Q \equiv (i\Omega_l, \mathbf{q})$ ,  $\sum_Q \equiv T \sum_l \sum_{\mathbf{q}}$ , etc., with  $\omega_n$  ( $\Omega_l$ ) being odd (even) Matsubara frequencies. Here  $\varphi_{\mathbf{k}}^*$  is the complex conjugate of  $\varphi_{\mathbf{k}}$ .

We emphasize that the derivation of this theory is independent of the concrete form of the pairing interaction, namely, it is not essential whether the interaction is  $s$  wave,  $p$  wave, or  $d$  wave, short range or long range, provided that one can assume a separable potential in the scattering  $T$  matrix [28]. In fact, the original zero-temperature BCS-BEC crossover by Leggett was done with  $p$ -wave pairing [29].

Due to the anisotropy of the DDI, the pair dispersion acquires an anisotropy as well, in contrast to the short-range contact potential case in a two-component Fermi gas. Namely, the finite  $\mathbf{q}$  pair propagator  $t_{pg}(Q)$  can be expanded as

$$t_{pg}^{-1}(Q) = Z(i\Omega_l - \Omega_{\mathbf{q}} + \mu_{\text{pair}} + i\Gamma_{\Omega, \mathbf{q}}), \quad (3)$$

with an effective pair dispersion  $\Omega_{\mathbf{q}} = \mathbf{q}_{\perp}^2 / (2M_{\perp}^*) + q_z^2 / (2M_z^*)$  and an effective pair chemical potential  $\mu_{\text{pair}}$ . Here

the inverse residue  $Z$  and the (anisotropic) effective pair mass  $M_{\perp}^* = M_x^* = M_y^*$  and  $M_z^*$  can be determined in the process of Taylor expansion, as usual. Following Ref. [17],  $\Sigma_{pg}$  can be approximated as  $\Sigma_{pg}(K) \approx -\Delta_{pg}^2 G_0(-K) |\varphi_{\mathbf{k}}|^2$ . With the odd parity  $\varphi_{-\mathbf{k}} = -\varphi_{\mathbf{k}}$ , here we have defined the pseudogap  $\Delta_{pg}$  as

$$\Delta_{pg}^2 = -2 \sum_Q t_{pg}(Q) \approx 2Z^{-1} \sum_{\mathbf{q}} b(\Omega_{\mathbf{q}}), \quad (4)$$

where  $b(x)$  is the Bose distribution function. This leads to the BCS form of the total self-energy,

$$\Sigma(K) = \Sigma_{sc}(K) + \Sigma_{pg}(K) = -\Delta^2 G_0(-K) |\varphi_{\mathbf{k}}|^2, \quad (5)$$

with a total excitation gap  $\Delta = \sqrt{\Delta_{sc}^2 + \Delta_{pg}^2}$ .

As in Ref. [17], from the Thouless criteria,  $t^{-1}(0, \mathbf{0}) = 0$ , we have the gap equation

$$1 + g \sum_{\mathbf{k}} \frac{1 - 2f(E_{\mathbf{k}})}{2E_{\mathbf{k}}} |\varphi_{\mathbf{k}}|^2 = 0, \quad (6)$$

and the fermion number equation

$$n = \sum_K G(K) = \sum_{\mathbf{k}} \left[ \frac{1}{2} \left( 1 - \frac{\xi_{\mathbf{k}}}{E_{\mathbf{k}}} \right) + \frac{\xi_{\mathbf{k}}}{E_{\mathbf{k}}} f(E_{\mathbf{k}}) \right], \quad (7)$$

where  $E_{\mathbf{k}} = \sqrt{\xi_{\mathbf{k}}^2 + \Delta^2 |\varphi_{\mathbf{k}}|^2}$  is the Bogoliubov quasiparticle dispersion and  $f(x)$  the Fermi distribution function.

Now we determine the symmetry factor  $\varphi_{\mathbf{k}}$  from the DDI,

$$V_d(\mathbf{r}) = d^2 \frac{1 - 3 \cos^2 \theta_{\mathbf{r}}}{r^3} = V(r) Y_{2,0}(\theta_{\mathbf{r}}, \phi_{\mathbf{r}}), \quad (8)$$

where the radial part  $V(r) = -\sqrt{16\pi/5} d^2 / r^3$ , and the angular part  $Y_{2,0}(\theta_{\mathbf{r}}, \phi_{\mathbf{r}})$  is the spherical harmonic  $Y_{lm_l}(\hat{\mathbf{r}})$ , with  $\theta_{\mathbf{r}}$  and  $\phi_{\mathbf{r}}$  the polar and azimuthal angles of  $\mathbf{r}$ . So the DDI breaks SO(3) symmetry and mixes different partial waves. Expanding  $V_{\mathbf{k}, \mathbf{k}'}$  in terms of partial waves, we have  $V_{\mathbf{k}, \mathbf{k}'} = \sum_{l'l'} \sum_{m_l m_{l'}} g_{m_l m_{l'}}^{ll'}(k, k') Y_{lm_l}(\hat{\mathbf{k}}) Y_{l'm_{l'}}^*(\hat{\mathbf{k}'})$ , with  $g_{m_l m_{l'}}^{ll'}(k, k') = (-1)^{\frac{l+l'}{2}} 16\pi^2 w_{l,l'}(k, k') \langle l m_l | Y_{20} | l' m_{l'} \rangle$  and  $w_{l,l'}(k, k') = \int_0^{\infty} r^2 dr j_l(kr) V(r) j_{l'}(k'r)$ , where  $j_l(kr)$  is the spherical Bessel function. For a single-component Fermi gas, only odd  $l$  and  $l'$  are allowed, with  $l' = l, l \pm 2$ . The  $r^{-3}$  dependence of the DDI leads to a  $k$ -independent  $w_{l,l'}(k, k)$ . Detailed analyses show that the dominant attractive channel in  $V_{\mathbf{k}, \mathbf{k}}$  is  $l = 1, m_l = 0$ , i.e., the  $p_z$  wave, where  $g_{00}^{11}(k, k) < 0$  is the leading order term, with  $g_{00}^{33}(k, k) \approx 0.1 g_{00}^{11}(k, k)$  being the next leading order term. The leading hybridization terms with  $l = 1, l' = 3$  are repulsive. Therefore here we concentrate on the  $p_z$ -wave channel.

To remove the ultraviolet divergence in the momentum integral of the gap equation, caused by the  $k$  independence of  $w_{l,l'}(k, k)$ , we regularize the DDI by multiplying a convergence factor  $F(r/r_0)$ , where  $r_0$  is the typical radius beyond which the DDI becomes dominant [30]. We choose  $F(x) = 1 - e^{-x}(1 + x + x^2/2)$ , similar to that used in Ref. [15] but here the regularized DDI approaches a finite value as  $r \rightarrow 0$ , as shown

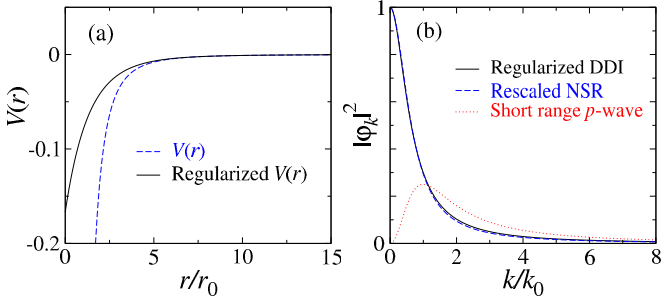


FIG. 2. (a) Radial part,  $V(r)$ , and regularized  $V(r)$  of the DDI, in units of  $\sqrt{16\pi/5}d^2$ . (b)  $k$  dependence of  $|\varphi_{\mathbf{k}}|^2$  calculated from the regularized DDI (black solid line) and  $|\varphi_{\mathbf{k}}|_{\text{NSR}}^2$  (blue dashed). For comparison, the radial part of a short-range interaction induced  $p$  wave  $|\varphi_{\mathbf{k}}|_p^2$ , which scales as  $k^2$  in the low energy limit, is plotted as well (red dotted).

in Fig. 2(a). This leads to a modified  $p_z$ -wave symmetry factor

$$\varphi_{\mathbf{k}}^2 = \frac{1}{2\eta^2} \left[ 1 - \frac{\ln(1 + 4\eta^2)}{4\eta^2} \right] \cos^2 \theta_{\mathbf{k}}, \quad (9)$$

where  $\varphi_{\mathbf{k}}$  is real, with  $\eta = k/k_0 = kr_0$ , and  $\theta_{\mathbf{k}}$  the polar angle of  $\mathbf{k}$ . Interestingly, the  $k$  dependence of this  $\varphi_{\mathbf{k}}$  is quantitatively very close to a rescaled  $s$ -wave Lorentzian symmetry factor used in Ref. [26],

$$\varphi_{\mathbf{k}}^2|_{\text{NSR}} = \frac{1}{1 + (1.55k/k_0)^2}, \quad (10)$$

as shown in Fig. 2(b). For comparison, we also plot the  $k$  dependence of a typical  $p$ -wave symmetry factor,  $|\varphi_{\mathbf{k}}|_p^2 = \frac{(k/k_0)^2}{[1 + (k/k_0)^2]^2}$ , induced by a short-range interaction [31–33], for which the partial wave scattering amplitude  $f_k^l \sim V_{kk} \sim |\varphi_{\mathbf{k}}|^2 \sim a_l k^{2l}$  as  $k \rightarrow 0$  so that for  $l = 1$ ,  $a_1$  is the scattering volume. *In contrast, the behavior of the  $p_z$ -wave scattering amplitude of the DDI is very similar to the short-range  $s$ -wave case, giving rise to a well-defined scattering length rather than scattering volume.* Indeed, the strict  $V(r)$  gives rise to a completely  $k$  independent scattering amplitude [8,34], as is the  $k_0 \rightarrow +\infty$  limit of Eq. (9).

Now with  $\varphi_{\mathbf{k}}$  given by Eq. (9) for the DDI, Eqs. (4), (6), and (7) form a closed set, which can be solved self-consistently for  $T_c$  as a function of the  $p$ -wave pairing strength,  $g = -24\pi D/(5m)$ , and for gaps below  $T_c$  as a function of  $T$ , where  $D = md^2/2$  is the dipole length. The unitary limit corresponds to the critical coupling strength  $g_c = -18\pi/(mk_0)$ , at which the scattering length diverges, and a bound state starts to form, as determined by the Lippmann-Schwinger equation [31,35]  $g_c^{-1} = -\sum_{\mathbf{k}} |\varphi_{\mathbf{k}}|^2 / (2\epsilon_{\mathbf{k}})$ , with  $\epsilon_{\mathbf{k}} = \mathbf{k}^2/(2m)$ . Thus  $g/g_c = 4k_0 D/15$ . In our numerical calculations we take  $k_0/k_F = 20$ , corresponding to a dilute case.

### III. NUMERICAL RESULTS AND DISCUSSIONS

We first present in Fig. 3 the calculated superfluid transition temperature  $T_c$  and corresponding  $\mu$  and pseudogap  $\Delta_{\text{pg}}$  at  $T_c$  as a function of pairing strength, which are obtained by setting  $\Delta_{\text{sc}} = 0$ . For comparison, the mean-field solution  $T_c^{\text{MF}}$  is also shown in Fig. 3(a) (red dashed curve). In the

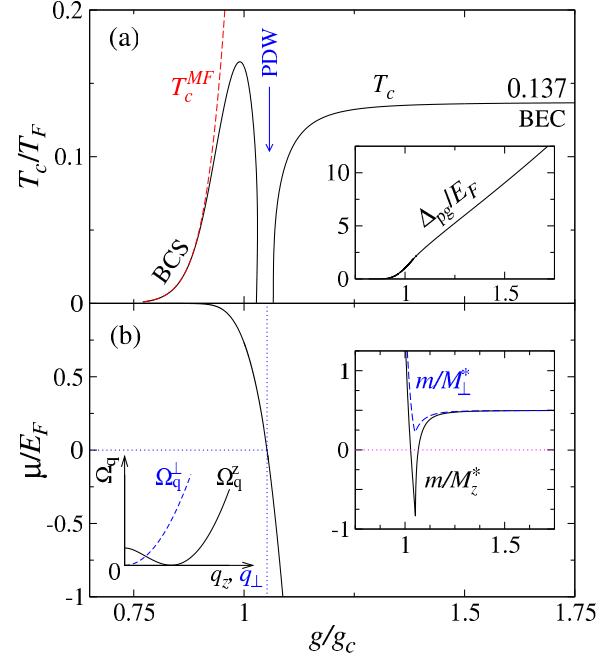


FIG. 3. (a) Superfluid transition temperature  $T_c$  (black solid curve), the mean-field  $T_c^{\text{MF}}$  (red dashed curve) and (b) chemical potential  $\mu(T_c)$  as a function of  $g/g_c$ . Shown in the insets are the pseudogap  $\Delta_{\text{pg}}(T_c)$  and the inverse pair mass  $m/M^*$ . A PDW state emerges where  $T_c$  shuts off at intermediate coupling strength and the inverse pair mass  $m/M_z^*$  becomes negative. The right insets share the same horizontal axis as the main panels. The lower left inset shows schematic pair dispersion in the PDW regime. While the inverse mass remains positive in the  $xy$  plane (blue dashed line), it becomes negative in the  $z$  direction (black solid curve), with a minimum at finite  $q_z$  in  $\Omega_{\mathbf{q}}^z$ .

weak-coupling regime,  $T_c$  follows the mean-field BCS result. It starts to decrease after it reaches a maximum around unitarity  $g/g_c = 1$ , due to the shrinking Fermi surface. Remarkably, it exhibits a reentrant behavior. For a range of intermediate pairing strength,  $T_c$  shuts off completely, before it recovers at stronger couplings, where the system has entered the BEC regime and all fermions are paired, with  $\mu < 0$ . With  $M^*$  approaching  $2m$  and  $n_{\text{pair}} = n/2$ ,  $T_c$  approaches the BEC asymptote,  $0.137T_F$ , from below. The pseudogap at  $T_c$  increases monotonically with  $g/g_c$ .

In order to understand the reentrant  $T_c$  behavior, we plot the inverse pair masses in the lower inset of Fig. 3(b). It reveals that, when  $T_c$  vanishes at the intermediate pairing strength, the effective pair mass in the dipole direction,  $M_z^*$ , at zero momentum becomes negative, so that the pair dispersion  $\Omega_{\mathbf{q}}$  in the  $\hat{z}$ -direction becomes rotonlike [36], with a minimum at a finite  $q_z$ , as shown schematically in the lower left inset of Fig. 3 (solid curve). The pair mass in the  $xy$  plane remains positive. This corresponds to a pair density wave ground state, with a crystallization wave vector  $q_z$  in the  $\hat{z}$  direction. Similar PDW states were extensively investigated in high- $T_c$  superconductors in the quasi-2D context [20,21].

We emphasize that *the nonmonotonic behavior of  $T_c$  as a function of pairing strength, as found in our  $T$ -matrix approach of the pairing fluctuation theory [17], can be under-*

stood on physical grounds, without invoking specific details of the theory. Indeed, this approach has been accepted by increasingly more researchers [37,38]. In the weak-coupling regime,  $T_c$  follows the mean-field behavior. As the pairing strength increases towards unitarity, the chemical potential decreases, leading to a shrinking Fermi surface and thus a decreasing density of state (DOS)  $N(0) \propto \sqrt{\mu}$ . At the same time, a pseudogap develops gradually due to strong pairing correlations, which causes a further depletion of the DOS at the Fermi level. Both these effects cause a reduction of  $T_c$ , as one can naively expect from the BCS formula for  $T_c$ . Such effects will reach their utmost when the Fermi surface disappears completely at  $\mu = 0$ . Therefore, it is natural to have a maximum of  $T_c$  within the fermionic regime. The actual position of the maximum depends largely on the range of the pairing interaction, and is close to unitarity in the contact potential limit. On the other hand, as the pseudogap develops, fermions form pairs. Upon entering the bosonic regime, essentially all fermions are paired. The BEC temperature of these pairs increases with the pairing strength, as the pair density does. This explains why the combined  $T_c$  exhibits a minimum around  $\mu = 0$ . At this point, the effective pair mass  $M^*$  is significantly heavier than  $2m$ , due to the repulsive interaction between pairs. As the pairing strength increases further into the BEC regime, the pair size shrinks, and the interpair scattering length decreases, so that  $M^*$  decreases gradually towards  $2m$ . As a consequence, the Bose condensation temperature  $T_c$  of the pairs necessarily increases towards its BEC asymptote from below. Within a  $T$ -matrix approximation, these arguments are independent of the specific form of the pair susceptibility.

We note that the emergence of the PDW state has to do with the long-range nature of the DDI, which essentially put the system in the high density regime. At the same time, due to the  $p_z$  symmetry, the coherence length  $\xi \sim v_F/\Delta_{\mathbf{k}}$  diverges in the nodal  $xy$  plane (i.e.,  $k_z = 0$ ) so that the order parameter  $\Delta_{\mathbf{k}} = \Delta\varphi_{\mathbf{k}}$  exhibits a nonlocal effect similar to the case of a  $d_{x^2-y^2}$ -wave superconductor [23]. (Here  $v_F$  is the Fermi velocity). Such a diverging in-plane coherence length makes it difficult for the pairs to move in the  $\hat{z}$  direction, without heavily colliding with other pairs. At certain intermediate interaction strength, pairing is strong while the pair size is large, so that the repulsive interaction between pairs becomes strong. Indeed, a careful look at the effective inverse pair mass reveals that before entering the PDW state, the pair mass already becomes heavy due to strong pair-pair repulsion. Therefore, the kinetic energy of the pairs (in the  $\hat{z}$  direction) becomes much smaller than the growing potential energy between pairs, in favor of forming a Wigner-like crystal structure, which is what we call the PDW state. Formation of such a crystal structure and minimization of the pair dispersion at a finite momentum suppress the superfluid  $T_c$  down to zero. Such a periodic crystal structure of a PDW state can be most directly probed using Bragg scattering, similar to the x-ray diffraction of a crystal structure of a solid.

To further test this picture, we plotted in Fig. 4 the  $T_c$  behavior of the finite range  $p_z$ -wave superfluid, with a pairing symmetry factor given by  $|\varphi_{\mathbf{k}}|_p \cos \theta_{\mathbf{k}}$ , as a function of pairing strength for representative values of the range of interaction, as given by  $k_0/k_F = 2.5$  and 1.0. Here  $k_F/k_0$  serves as the

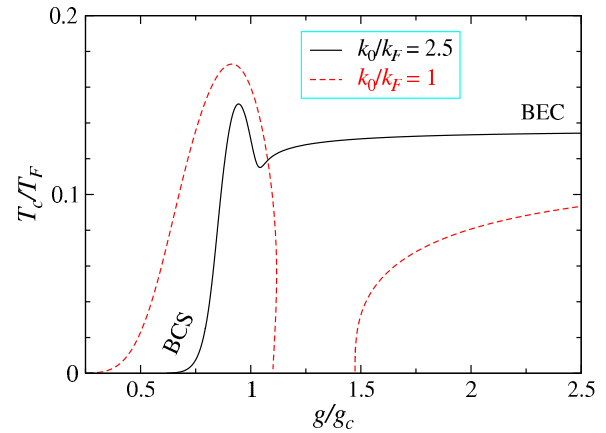


FIG. 4.  $T_c$  behavior of a finite range  $p_z$ -wave superfluid as a function of  $g/g_c$  for  $k_0/k_F = 2.5$  (black solid) and 1.0 (red dashed line). The pairing symmetry is given by  $|\varphi_{\mathbf{k}}|_p \cos \theta_{\mathbf{k}}$ .

effective range of interaction, in units of the interparticle distance ( $1/k_F$ ). For a short range,  $k_0/k_F = 2.5$ , the crossover is smooth and continuous, similar to a short-range  $s$ -wave case [39], except for a reduced BEC asymptote. As  $k_F/k_0$  increases, more particles are within the range of interaction at the same time so that the effective repulsion between pairs becomes strong and the pair mass becomes heavy. For a larger range,  $k_0/k_F = 1$ , a reentrant behavior of  $T_c$  appears, as in the dipole-dipole interaction case (and PDW states emerge where  $T_c$  vanishes). In fact, such reentrant behavior also occurs for  $s$ -wave pairing with a large range of interaction [28]. This supports our conclusion that the reentrant behavior of  $T_c$  for a dipolar Fermi gas results from the long-range nature of the DDI. We emphasize that the reentrant behavior is not unique to the DDI, nor is it to the  $p$ -wave pairing symmetry.

In the absence of an underlying lattice potential, the PDW state in the dipolar Fermi gases is distinct from a Mott state. Instead, it may exhibit behaviors of a Bose metal [24,25]. The presence of the PDW manifests a Bose “surface” for pair excitations [40], whose energy vanishes at a finite momentum  $q_z$  (with  $q_x = q_y = 0$ ). While the pair dispersion remains positive in the  $xy$  plane, the two dimensionality destroys the long-range superfluid order, leading to a metallic ground state with a density wave of Cooper pairs in the  $\hat{z}$  direction. The nature of the PDW state deserves further systematic investigations [41].

It should be mentioned that the chemical potential  $\mu$  changes sign within the PDW regime. In the fermionic regime, there is a line node at  $k_z = 0$  on the Fermi surface in the  $p_z$ -wave superfluid order parameter. Once  $\mu$  becomes negative, the node disappears and the excitation spectrum  $E_{\mathbf{k}}$  becomes fully gapped. This may be regarded as a topological transition [29,32]. The anisotropy in the pair mass is a consequence of the DDI. We emphasize that the reentrant behavior of  $T_c$  is robust against changes of  $k_0$  and independent of the regularization scheme, because  $k_0$  does not modify the long-range part of the DDI. It is also present in the next leading order,  $f_z$ -wave channel.

Note that when  $\mu$  changes sign, the pairing gap  $\Delta$  is rather large (of the order  $E_F$ ). There exists an extended range of low

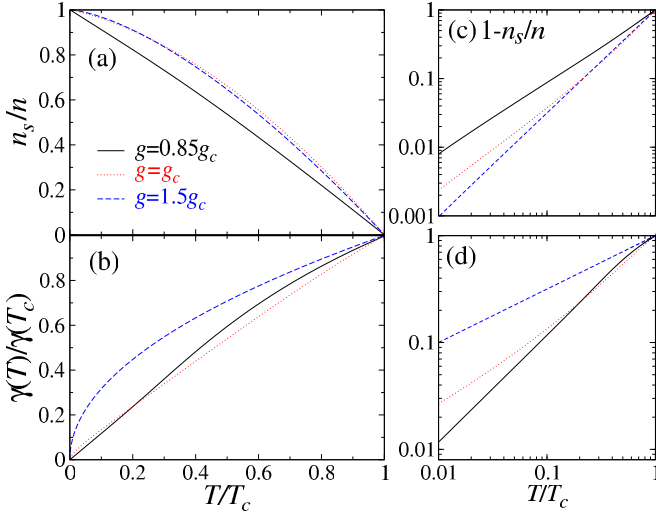


FIG. 5. Transport and thermodynamic behavior. (a)  $n_s/n$  and (b)  $\gamma(T)/\gamma(T_c)$  as a function of  $T/T_c$  for  $g/g_c = 0.85$  (BCS), 1.0 (unitary), and 1.5 (BEC), and log-log plot of (c)  $1 - n_s/n$  and (d)  $\gamma(T)/\gamma(T_c)$  vs  $T/T_c$ .

$T \ll \Delta$ , where  $\mu$ ,  $\Delta$ , and  $M^*$  remain essentially constant, so that the PDW state is rather insensitive to  $T$  in this temperature range.

For  $d$ -wave pairing as in the cuprates,  $T_c$  vanishes at a lower critical doping concentration, for which the calculated effective pair mass diverges as well. Below this doping concentration, the pair dispersion acquires a minimum at a finite momentum, with a negative mass at  $q = 0$ . This suggests that the PDW in the cuprates and the PDW in the dipolar Fermi gases may share the same origin.

Next we investigate the transport and thermodynamics behavior in the superfluid phase. The superfluid density can be derived using a linear response theory. Following Ref. [17], we obtain

$$n_s = \frac{m\Delta_{sc}^2}{3} \sum_{\mathbf{k}} \frac{1}{E_{\mathbf{k}}^2} \left[ \frac{1 - 2f(E_{\mathbf{k}})}{2E_{\mathbf{k}}} + f'(E_{\mathbf{k}}) \right] \times \left[ (\nabla_{\mathbf{k}} \xi_{\mathbf{k}})^2 |\varphi_{\mathbf{k}}|^2 - \frac{1}{4} (\nabla_{\mathbf{k}} \xi_{\mathbf{k}}^2) \cdot (\nabla_{\mathbf{k}} |\varphi_{\mathbf{k}}|^2) \right], \quad (11)$$

where  $f'(x) = df(x)/dx$ . It can be shown that  $n_s(0) = n$ . At  $0 < T \leq T_c$ , both Bogoliubov quasiparticles and pair excitations contribute to the thermodynamics. This leads to the specific heat  $C_v = \sum_{\mathbf{k}} E_{\mathbf{k}} \partial_T f(E_{\mathbf{k}}) + \sum_{\mathbf{q}} \Omega_{\mathbf{q}} \partial_T b(\Omega_{\mathbf{q}})$ .

Shown in Fig. 5 are the  $T$  dependencies of (a)  $n_s$  and (b)  $\gamma = C_v/T$ , for  $g/g_c = 0.85, 1.0$ , and  $1.5$ , corresponding to BCS, unitary, and BEC regimes, respectively. These two quantities are sensitive to the elementary excitation spectrum. Due to the line node on the Fermi surface of the  $p_z$ -wave superfluid, the low energy density of states  $N(E)$  is linear in  $E$ . Therefore, the low  $T$  superfluid density and specific heat exhibit power laws in contrast to the exponential behavior of an  $s$ -wave superfluid. In the BCS regime, both the low temperature normal-fluid density  $n_n/n = 1 - n_s/n$  and  $\gamma(T)$  are linear in  $T$ , similar to their counterpart in the nodal  $d$ -wave cuprate superconductors. On the other hand, in the BEC regime, pair excitations dominate, so that  $n_n/n \sim (T/T_c)^{3/2}$  and

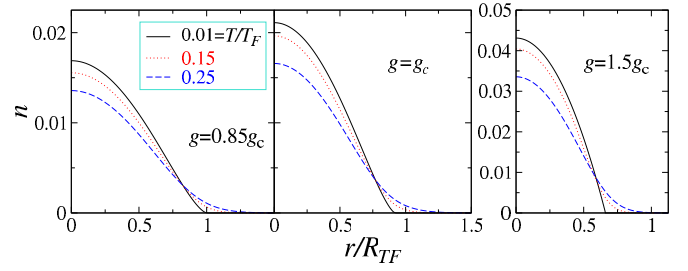


FIG. 6. Comparison of density profiles in an isotropic harmonic trap at  $T/T_F = 0.01, 0.15$ , and  $0.25$  and pairing strengths  $g/g_c = 0.85$  (BCS), 1.0 (unitary), and 1.5 (BEC). Here  $R_{TF}$  is the Thomas-Fermi radius and the density  $n$  is in units of  $k_F^3$ .

$\gamma \sim (T/T_c)^{1/2}$ , similar to the short-range  $s$ -wave case. At  $g = g_c$ , both types of excitations coexist, and thus the  $T$  dependence exhibits a crossover. The power-law behaviors are best manifested in log-log plots, as slope changes in Figs. 5(c) and 5(d). While the qualitative features shown here may be easily anticipated, we emphasize that this is the first systematic study of the thermodynamic behavior of a superfluid of a dipolar Fermi gas throughout the BCS-BEC crossover.

Finally, we consider the effect of a 3D isotropic harmonic trap of frequency  $\omega$  with a trapping potential  $V_{\text{trap}}(\mathbf{r}) = \frac{1}{2}m\omega^2 r^2$ . We assume that  $E_F$  is large enough to justify the use of LDA [38,42]. Then  $\mu$  is replaced by  $\mu(\mathbf{r}) = \mu_0 - V_{\text{trap}}(\mathbf{r})$ , where the global chemical potential  $\mu_0$  is determined by the total fermion number constraint,  $N = \int_{\text{trap}} n(\mathbf{r}) d^3r$ , with local density  $n(\mathbf{r})$ . Outside the superfluid core, a nonvanishing  $\mu_{\text{pair}}(r)$  is included so that the gap and the pseudogap equations are extended as  $t^{-1}(0, \mathbf{0}) = Z\mu_{\text{pair}}$  and  $\Delta_{\text{pg}}^2 = 2Z^{-1} \sum_{\mathbf{q}} b(\Omega_{\mathbf{q}} - \mu_{\text{pair}})$ , respectively. Shown in Fig. 6 is the evolution of the density profile from low to high  $T$ , throughout the BCS-BEC crossover. Despite the anisotropic pairing interaction, the density profile remains isotropic under LDA. It broadens with increasing temperature, whereas it shrinks with increasing DDI strength, similar to its  $s$ -wave counterpart with a contact potential [42]. The isotropic density profile partly reflects the fact that (i) the pairing symmetry becomes internal degrees of freedom for the fermion pairs and (ii) within the LDA, this isotropy comes from the isotropic  $V_{\text{trap}}(r)$ . Possible anisotropy in the density profile may occur when direct pair-pair interactions beyond the  $T$ -matrix level are included, without using the LDA.

Recent studies [43–45], using Hartree-Fock approximation, suggest that the normal state 3D dipolar Fermi gas is subject to collapse and phase separation instabilities in the high density and strong DDI regime. For the dilute case considered in the present work, the Hartree-Fock contribution to the system energy, proportional to  $n^2$ , is relatively weak. Our calculations show that, within the  $T$ -matrix approximation, the compressibility for paired superfluid phase at  $T \leq T_c$  remains positive definite throughout the BCS-BEC crossover, ensuring a stable superfluid state. Effects of direct pair-pair interactions beyond the  $T$ -matrix approximation will be investigated in a future study.

## IV. CONCLUSIONS

In summary, our study of single-component dipolar Fermi gases reveals a reentrant behavior of a  $p_z$ -wave superfluid transition  $T_c$  and a PDW state in a range of intermediate DDI strength. Such a PDW state as well as the  $p_z$ -wave superfluid phase may be detected using local density measurements, Bragg spectroscopy, and momentum resolved rf spectroscopy.

## ACKNOWLEDGMENTS

We thank Hui Zhai, Wei Yi, Xin Wan, Hua Chen, and K. Levin for helpful discussions. This work is supported by NSF of China (Grants No. 10974173 and No. 11274267), the National Basic Research Program of China (Grants No. 2011CB921303 and No. 2012CB927404), and NSF of Zhejiang Province of China (Grant No. LZ13A040001).

- 
- [1] M. Lu, N. Q. Burdick, and B. L. Lev, *Phys. Rev. Lett.* **108**, 215301 (2012).
- [2] B. Naylor, A. Reigue, E. Maréchal, O. Gorceix, B. Laburthe-Tolra, and L. Vernac, *Phys. Rev. A* **91**, 011603 (2015).
- [3] K. Aikawa, A. Frisch, M. Mark, S. Baier, R. Grimm, and F. Ferlaino, *Phys. Rev. Lett.* **112**, 010404 (2014).
- [4] K. K. Ni, S. Ospelkaus, M. H. G. de Miranda, A. Pe'er, B. Neyenhuis, J. J. Zirbel, S. Kotochigova, P. S. Julienne, D. S. Jin, and J. Ye, *Science* **322**, 231 (2008).
- [5] C.-H. Wu, J. W. Park, P. Ahmadi, S. Will, and M. W. Zwierlein, *Phys. Rev. Lett.* **109**, 085301 (2012).
- [6] J. W. Park, S. A. Will, and M. W. Zwierlein, *Phys. Rev. Lett.* **114**, 205302 (2015).
- [7] L. You and M. Marinescu, *Phys. Rev. A* **60**, 2324 (1999).
- [8] M. A. Baranov, M. S. Mar'enko, V. S. Rychkov, and G. V. Shlyapnikov, *Phys. Rev. A* **66**, 013606 (2002).
- [9] B. Liu, X. Li, L. Yin, and W. V. Liu, *Phys. Rev. Lett.* **114**, 045302 (2015).
- [10] C. J. Wu and J. E. Hirsch, *Phys. Rev. B* **81**, 020508(R) (2010).
- [11] Y. Li and C. J. Wu, *J. Phys.: Condens. Matter* **26**, 493203 (2014).
- [12] N. R. Cooper and G. V. Shlyapnikov, *Phys. Rev. Lett.* **103**, 155302 (2009).
- [13] X.-L. Qi and S.-C. Zhang, *Rev. Mod. Phys.* **83**, 1057 (2011).
- [14] K. K. Ni, S. Ospelkaus, D. Wang, G. Quemener, B. Neyenhuis, M. H. G. de Miranda, J. L. Bohn, J. Ye, and D. S. Jin, *Nature (London)* **464**, 1324 (2010).
- [15] R. Qi, Z.-Y. Shi, and H. Zhai, *Phys. Rev. Lett.* **110**, 045302 (2013).
- [16] T. Shi, S.-H. Zou, H. Hu, C.-P. Sun, and S. Yi, *Phys. Rev. Lett.* **110**, 045301 (2013).
- [17] Q. J. Chen, I. Koztlin, B. Jankó, and K. Levin, *Phys. Rev. Lett.* **81**, 4708 (1998).
- [18] Q. J. Chen, J. Stajic, S. Tan, and K. Levin, *Phys. Rep.* **412**, 1 (2005).
- [19] Q. J. Chen and J. B. Wang, *Front. Phys.* **9**, 539 (2014).
- [20] Z. Tešanović, *Phys. Rev. Lett.* **93**, 217004 (2004).
- [21] H.-D. Chen, O. Vafek, A. Yazdani, and S.-C. Zhang, *Phys. Rev. Lett.* **93**, 187002 (2004).
- [22] L. A. Sidorenkov, M. K. Tey, R. Grimm, Y.-H. Hou, L. Pitaevskii, and S. Stringari, *Nature (London)* **498**, 78 (2013).
- [23] I. Koztlin and A. J. Leggett, *Phys. Rev. Lett.* **79**, 135 (1997).
- [24] D. Das and S. Doniach, *Phys. Rev. B* **60**, 1261 (1999); **64**, 134511 (2001).
- [25] H.-H. Lai, K. Yang, and N. E. Bonesteel, *Phys. Rev. Lett.* **111**, 210402 (2013).
- [26] P. Nozières and S. Schmitt-Rink, *J. Low Temp. Phys.* **59**, 195 (1985).
- [27] L. P. Kadanoff and P. C. Martin, *Phys. Rev.* **124**, 670 (1961).
- [28] Q. J. Chen, Ph.D. thesis, University of Chicago, 2000.
- [29] A. J. Leggett, *Modern Trends in the Theory of Condensed Matter* (Springer-Verlag, Berlin, 1980), pp. 13–27.
- [30] This regularization is justified in that the actual interaction necessarily deviates from the strict DDI at a distance closer than or comparable to the size of the atoms (or molecules).
- [31] T.-L. Ho and R. B. Diener, *Phys. Rev. Lett.* **94**, 090402 (2005).
- [32] M. Iskin and C. A. R. Sá de Melo, *Phys. Rev. Lett.* **96**, 040402 (2006).
- [33] Y. Ohashi, *Phys. Rev. Lett.* **94**, 050403 (2005).
- [34] M. Marinescu and L. You, *Phys. Rev. Lett.* **81**, 4596 (1998).
- [35] C. J. Pethick and H. Smith, *Bose Einstein Condensation in Dilute Gases* (Cambridge University Press, Cambridge, 2002).
- [36] L. Santos, G. V. Shlyapnikov, and M. Lewenstein, *Phys. Rev. Lett.* **90**, 250403 (2003); A. Boudjemâa and G. V. Shlyapnikov, *Phys. Rev. A* **87**, 025601 (2013).
- [37] J. Kinnunen, M. Rodriguez, and P. Törmä, *Science* **305**, 1131 (2004); T. Ozawa and G. Baym, *Phys. Rev. A* **82**, 063615 (2010); X. S. Yang, B. B. Huang, and S. L. Wan, *Eur. Phys. J. B* **83**, 445 (2011); L. Y. He, X.-G. Huang, H. Hu, and X.-J. Liu, *Phys. Rev. A* **87**, 053616 (2013).
- [38] W. Yi and L.-M. Duan, *Phys. Rev. A* **73**, 031604(R) (2006).
- [39] Note that the location of the maximum  $T_c$  depends on  $k_0/k_F$ . Only in the  $k_0 \rightarrow +\infty$  limit does the maximum occur at  $g/g_c = 1$ .
- [40] S. Sachdev, *Nature (London)* **418**, 739 (2002); A. Paramekanti, L. Balents, and M. P. A. Fisher, *Phys. Rev. B* **66**, 054526 (2002).
- [41] The zero  $T$  inverse pair mass in the PDW state is extracted from the pairing  $T$  matrix, based on the mean-field solution of the gap  $\Delta$  and chemical potential  $\mu$ , since it is generally believed that the mean-field result is reasonably good for intermediate pairing strengths at  $T = 0$ . It remains to be seen whether such a PDW state is present in the  $GG$  scheme of the  $T$ -matrix approximation, with pair susceptibility  $\chi = GG$ .
- [42] Y. He, C.-C. Chien, Q. J. Chen, and K. Levin, *Phys. Rev. B* **76**, 224516 (2007).
- [43] T. Sogo, L. He, T. Miyakawa, S. Yi, H. Lu, and H. Pu, *New J. Phys.* **11**, 055017 (2009).
- [44] S. Ronen and J. L. Bohn, *Phys. Rev. A* **81**, 033601 (2010).
- [45] K. Sun, C. Wu, and S. Das Sarma, *Phys. Rev. B* **82**, 075105 (2010).